JOC Article

Structure−Property Relationships in Push−Pull Amino/Cyanovinyl End-Capped Oligothiophenes: Quantum Chemical and Experimental Studies

María Moreno Oliva,[†] Juan Casado,[†] M. Manuela M. Raposo,[‡] A. Maurício C. Fonseca,[‡] Horst Hartmann,[§] Víctor Hernández,[†] and Juan T. López Navarrete*[,†]

Department of Physical Chemistry, University of Málaga, 29071 Málaga, Spain, Centro de Química, Universidade do Minho, Campus de Gualtar, 4710-057 Braga, Portugal, and Fachbereich Chemie der Fachhochschule Merseburg, Geusaer Strasse, D-06217 Merseburg, Germany

teodomiro@uma.es

Received February 15, 2006

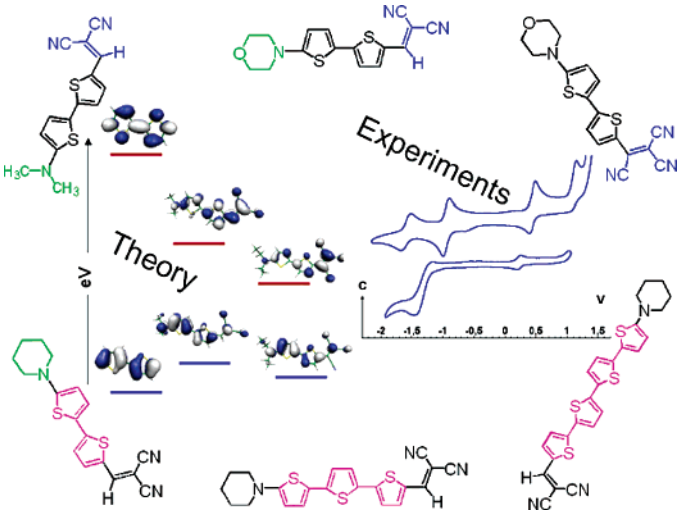

A series of push−pull chromophores built around thiophene-based π-conjugating spacers and bearing various types of amino donors and cyanovinyl acceptors have been analyzed by means of UV−vis−NIR, IR, and Raman spectroscopic measurements in the solid state as well as in solution. The intramolecular charge transfer (ICT) of these π-conjugated systems has also been tested by analyzing the ability of the solute molecules to undergo shifts in their fluorescence emission maxima with increasing solvent polarity. These push−pull oligomers also display an attractive electrochemical behavior since they generate stable species both upon oxidation and reduction. Oxidation mainly involves changes in the electron-rich aminooligothienyl half-part of the molecule and leads to the formation of stable cations. On the other hand, reduction to radical anions and dianions is mainly cyanovinyl-centered but also affects the π-conjugated electron relay. Density functional theory (DFT) calculations have been carried out to help the assignment of the most relevant electronic and vibrational features and to derive useful information about the molecular structure of these NLO-phores.

I. Introduction

Low band gap polyconjugated organic polymers are quite attractive materials for their applicability in the fabrication of high performance optical and electronic devices.[1] At present, the synthesis of oligomers with well-defined substitution patterns and chain lengths constitutes an alternative way to overcome the problems inherent to the polydispersity and common insolubility of polymers.[2] The ability of the π-conjugated oligomers as chromophores and electrophores is related to the

[†] University of Málaga.
[‡] Universidade do Minho.
[§] Fachbereich Chemie der Fachhochschule Merseburg.

10.1021/jo060318v CCC: $33.50
Published on Web 09/02/2006

efficiency of the intramolecular delocalization of π-electrons along the molecular long axis. Thus, one of the main challenges of the research of this class of materials is to investigate the relevant properties of extensively conjugated chains as a function of the so-called "effective conjugation length", qualitatively defined as the length of the molecular domain over which π-delocalization takes place.[3]

Electrooptic materials with potential use in photonic devices for telecommunications and optical information processing[4] usually involve a host polymeric matrixes containing second-order nonlinear optical (NLO) chromophores either as guest molecules or covalently attached to the polymeric backbone. Dipolar push−pull chromophores constitute the widest class of compounds investigated for their NLO properties.[4−10] These push−pull NLO-phores are basically constituted by an electron donor (D) and an electron acceptor (A) group interacting through a π-conjugated spacer.

It is well recognized that the NLO activity of push−pull chromophores is determined not only by the strength of the D−A pair but also more subtly by the π-conjugated spacer.[5] When comparing typical spacers, such as polyenes, oligophenylenes, or oligothiophenes, of the same chain length and bearing the same D−A pair, a more pronounced red shift (in a given solvent) is commonly observed for the low-energy absorption maximum, λ_{max}, in polyenes than in oligophenylenes or oligothiophenes, indicative of an efficient electron transmission from the donor to the acceptor. The bathochromic shift of the visible absorption of the push−pull chromophore is even more intensified in high polar solvents. This positive solvatochromism has been commonly regarded as an indication of molecular nonlinearity ($\mu\beta$) of NLO-phores.[11−13] However, it was recently reported that some polyenes attached to a strong D−A pair display an inverted solvatochromism.[14,15] Their λ_{max} values exhibit a red shift with an increase of solvent polarity up to a certain polarity limit and then reverse this trend with a further increase of solvent polarity beyond that limit. Clearly, such spectroscopic behavior is not a simple attribute of the D−A strength but is also associated with the electronic properties of the π-conjugated spacer.

Although polyenic systems represent, in principle, the most effective way to achieve charge redistribution between the donor and the acceptor end groups, and D−A polyenes have been shown to exhibit huge nonlinearities,[5] the well-known limited chemical and photothermal stability of extended polyenes might represent an obstacle to the practical applications of the derived NLO-phores. With regards to oligophenylenes, the efficiency of electron transmission is limited by the large aromaticity of the benzene ring, which has a detrimental effect on the second-order polarizabilities. In comparison with oligophenylenes, oligothiophenes behave as very efficient electron relays almost comparable to polyenes,[5,16] because of the lower resonance energy of thiophene compared to that of benzene, and have been shown to give larger contributions to $\mu\beta(0)$.[12,17,18] Oligophenylenes attain a rapid saturation beyond the terphenyl unit, whereas oligothiophenes have a strong tendency to increase $\mu\beta(0)$ with increasing number of thiophene units. Aside from the electron transmission efficiency, another merit of oligothiophenes is their inherent stability from which thiophene-based D−A chromophores should benefit.[19,20]

(1) (a) *Handbook of Conducting Polymers*, 2nd ed.; Skotheim, T. A., Elsenbaumer, R. L., Reynolds, J. R., Eds.; Marcel Dekker: New York, 1998. (b) *Conjugated Polymers and Related Materials*; Salaneck, W. R., Lundstrom, I., Ranby, B., Eds.; Oxford University Press: Oxford, U.K., 1993.

(2) (a) *Electronic Materials: The Oligomeric Approach*; Müllen, K., Wegner, G., Eds.; Wiley-VCH: Weinheim, Germany, 1998. (b) *Handbook of Oligo and Polythiophenes*; Fichou, D., Ed.; Wiley-VCH: New York, 1999.

(3) (a) Hörold, H.-H.; Helbig, W. *Macromol. Chem., Macromol. Symp.* **1987**, *12*, 229. (b) Hörold, H.-H.; Offermann, J.; Atrat, P.; Tauer, K. D.; Drefahl, G. *Tr. Mezhdunar. Symp.* **1975**, 171; *Chem. Abstr. 85*, 124388.

(4) (a) Prasad, P. N.; Williams, D. J. *Introduction to Nonlinear Optical Effects in Molecules and Polymers*; Wiley: New York, 1991. (b) Zyss, J. *Molecular Nonlinear Optics*: *Materials, Physics and Devices*; Academic Press: Boston, 1993. (c) Kanis, D. R.; Ratner, M. A.; Marks, T. J. *Chem. Rev.* **1994**, *94*, 195. (d) Marder, S. R.; Perry, J. W. *Adv. Mater.* **1993**, *5*, 804. (e) Marks, T. J.; Ratner, M. A. *Angew. Chem., Int. Ed. Engl.* **1995**, *34*, 155. (f) Dalton, L. R.; Harper, A. W.; Ghosn, R.; Steier, W. H.; Ziari, M.; Fetterman, H.; Shi, Y.; Mustacich, R. V.; Jen, A. K.-Y.; Shea, K. J. *Chem. Mater.* **1995**, *7*, 1060. (g) Shi, Y.; Zhang, C.; Bechtel, J. H.; Dalton, L. R.; Robinson, B. H.; Steier, W. H. *Science* **2000**, *288*, 119. (h) Wolf, J.; Wortmann, R. *Adv. Phys. Org. Chem.* **1999**, *32*, 121. (i) Long, N. J. *Angew. Chem., Int. Ed. Engl.* **1995**, *34*, 21. (j) Brown, A. R.; Pomp, A.; Hart, C. M.; de Leeuw, D. M. *Science* **1995**, *270*, 972. (k) Friend, R. H.; Gymer, R. W.; Holmes, A. B.; Burroughes, J. H.; Marks, R. N.; Taliani, C.; Bradley, D. D. C.; Dos Santos, D. A.; Brèdas, J.-L.; Lögdlund, M.; Salaneck, W. R. *Nature* **1999**, *397*, 121.

(5) (a) Marder, S. R.; Gorman, C. B.; Tiemann, B. G.; Cheng, L. T. *J. Am. Chem Soc.* **1993**, *115*, 3006. (b) Marder, S. R.; Cheng, L. T.; Tiemann, B. G. *J. Chem. Soc., Chem. Commun.* **1992**, 672. (c) Marder, S. R.; Cheng, L. T.; Tiemann, B. G.; Friedli, A. C.; Blanchard-Desce, M.; Perry, J. W.; Skindhoj, J. *Science* **1994**, *263*, 511.

(6) (a) Mignani, G.; Leising, F.; Meyreux, R.; Samson, H. *Tetrahedron Lett.* **1990**, *31*, 4743. (b) Jen, A. K.-Y.; Rao, V. P.; Drost, K. J.; Wong, K. Y.; Cava, M. P. *J. Chem. Soc., Chem. Commun.* **1994**, 2057. (c) Rao, V. P.; Cai, Y. M.; Jen, A. K.-Y. *J. Chem. Soc., Chem. Commun.* **1994**, 1689.

(7) Rao, V. P.; Jen, A. K.-Y.; Wong, K. Y.; Drost, K. J. *J. Chem. Soc., Chem. Commun.* **1993**, 1118. (b) Gilmour, S.; Montgomery, R. A.; Marder, S. R.; Cheng, L.-T.; Jen, A. K.-Y.; Cai, Y.; Perry, J. W.; Dalton, L. R. *Chem. Mater.* **1994**, *6*, 1603. (c) Boldt, P.; Bourhill, G.; Bräuchle, C.; Jim, Y.; Kammler, R.; Müller, C.; Rase, J.; Wichern, J. *Chem. Commun*. **1996**, 793. (d) Wu, X.; Wu, J.; Liu, Y.; Jen, A. K.-Y. *J. Am. Chem. Soc*. **1999**, *121*, 472. (e) Wu, X.; Wu, J.; Liu, Y.; Jen, A. K.-Y. *Chem. Commun*. **1999**, 2391.

(8) (a) Sun, S.-S.; Zhang, C.; Dalton, L. R.; Garner, S. M.; Chen, A.; Steier, W. H. *Chem. Mater.* **1996**, *8*, 2539. (b) Jen, A. K.-Y.; Liu, Y.; Zheng, L.; Liu, S.; Drost, K. J.; Zhang, Y.; Dalton, L. R. *Adv. Mater*. **1999**, *11*, 452.

(9) (a) Rao, V. P.; Jen, A. K.-Y.; Wong, K. Y.; Drost, K. J. *Tetrahedron Lett.* **1993**, *34*, 1747. (b) Rao, V. P.; Cai, C.; Liakatas, I.; Wong, M.-S.; Bösch, M.; Bosshard, C.; Günter, P.; Concilio, S.; Tirelli, N.; Suter, U. W. *Org. Lett.* **1999**, *1*, 1847.

(10) (a) Marder, S. R.; Perry, J. W.; Bourhill, G.; Gorman, C. B.; Tiemann, B. G.; Mansour, K. *Science* **1993**, *261*, 186. (b) Marder, S. R.; Gorman, C. B.; Meyers, F.; Perry, J. W.; Bourhill, G.; Brédas, J.-L.; Pierce, B. M. *Science* **1994**, *265*, 632.

(11) (a) Barzoukas, M.; Blanchard-Desce, M.; Josse, D.; Lehn, J.-M.; Zyss, J. *Chem. Phys.* **1989**, *133*, 323. (b) Slama-Schowk, A.; Blanchard-Desce, M.; Lehn, J.-M. *J. Phys. Chem*. **1990**, *94*, 3894. (c) Blanchard-Desce, M.; Wortmann, R.; Lebus, S.; Lehn, J.-M.; Krämer, P. *Chem. Phys. Lett*. **1995**, *243*, 526. (d) Blanchard-Desce, M.; Runser, C.; Fort, A.; Barzoukas, M.; Lehn, J.-M.; Bloy, V.; Alain, V. *Chem. Phys.* **1995**, *199*, 253. (e) Verbiest, T.; Houbrechts, S.; Kauranen, M.; Clays, K.; Peersons, A. *J. Mater. Chem*. **1997**, *7*, 215. (f) Kim, O.-K.; Fort, A.; Barzoukas, M.; Blanchard-Desce, M.; Lehn, J.-M. *J. Mater. Chem*. **1999**, *9*, 2227.

(12) (a) Effenberger, F.; Würthner, F. *Angew. Chem., Int. Ed. Engl.* **1993**, *32*, 712. (b) Würthner, F.; Effenberger, F.; Wortmann, R.; Krämer, P. *Chem. Phys.* **1993**, *173*, 305. (c) Effenberger, F.; Würthner, F.; Steybe, F. *J. Org. Chem.* **1995**, *60*, 2082. (d) Steybe, F.; Effenberger, F.; Gubler, U.; Bosshard, C.; Günter, P. *Tetrahedron* **1998**, *54*, 8469.

(13) Cabrera, I.; Althoff, O.; Man, H.-T.; Yoon, H. N. *Adv. Mater.* **1994**, *6*, 43.

(14) Marder, S. R.; Perry, J. W.; Tiemann, B. G.; Gorman, C. B.; Gilmour, S.; Biddle, S. L.; Bourhill, G. *J. Am. Chem. Soc.* **1993**, *115*, 2524.

(15) Blanchard-Desce, M.; Alain, V.; Bedworth, P. V.; Marder, S. R.; Fort, A.; Runser, C.; Barzoukas, M.; Lebus, S.; Wortmann, R. *Chem.—Eur. J.* **1997**, *3*, 1091.

(16) (a) Rao, V. P.; Jen, A. K.-Y.; Cai, Y. *J. Chem. Soc., Chem. Commun.* **1996**, 1237. (b) Jen, A. K.-Y.; Cai, Y.; Bedworth, P. V.; Marder, S. R. *Adv. Mater*. **1997**, *9*, 132.

(17) Cheng, L.-T.; Tam, W.; Marder, S. R.; Stiegman, A. E.; Rikhen, G.; Spangler, C. W. *J. Phys. Chem.* **1991**, *95*, 10643.

(18) Ledoux, I.; Zyss, J.; Jutand, A.; Amatore, C. *Chem. Phys.* **1991**, *150*, 117.

(19) Gilmore, S.; Marder, S. R.; Perry, J. W.; Cheng, L.-T. *Adv. Mater.* **1994**, *6*, 494.

CHART 1. Parent Push−Pull Oligothienyl NLO-phores Considered in This Study

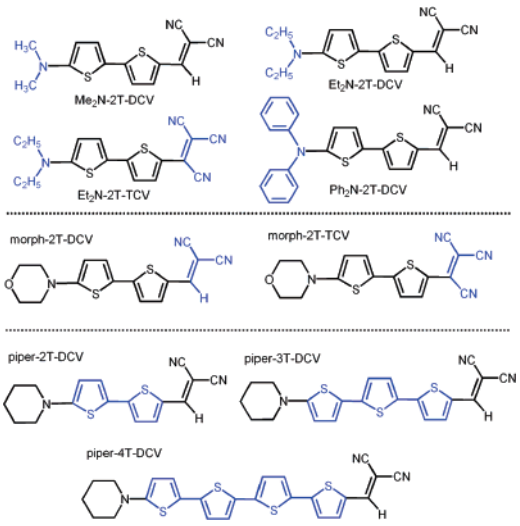

Some of us have recently reported on the synthesis of several donor−acceptor end-capped oligothiophenes bearing different 5-dialkylamino (D) and 5′-dicyanovinyl or 5′-tricyanovinyl (A) electroactive end groups with the scope of searching new solvatochromic dyes which could act as suited probes for the determination of solvent polarity or as materials with potential applications in NLO (Chart 1).[21] The longest wavelength optical absorptions of these thiophene-based push−pull chromophores are polarized along the long molecular axis and are strongly influenced by the chemical nature of the electron-withdrawing and electron-donating end groups. The bathochromic shift and ever-growing intensity with increasing donor and acceptor strength of the end groups are consistent with a charge-transfer (CT) character of this transition. The positive solvatochromic shift of the CT band of some of these push−pull bithiophenes extends almost over the whole visible range, indicating a large electronic interaction between the two α,α′-substituents and electron delocalization over the π-conjugated bridge.

Vibrational spectra of π-conjugated chain compounds constitute a very rich source of information on their structure. In particular, Raman spectra display characteristic features which are related to the strength and spatial extent of the electronic interactions between the successive chemical units along the chain, whose adequate interpretation has been required for the development over the past 15 years of new theoretical concepts.[22] In this regard, we would like to notice that infrared and Raman spectroscopies have also been successfully used as reliable methods to estimate the degree of charge transfer in TTF (tetrathiafulvalene)[23] and TCNQ (7,7,8,8-tetracyanoquinodimethane)[24] salts.

We have reported in recent years on a detailed vibrational study of the neutral,[25] radical cationic,[26] and dicationic[27] forms of a whole series of α,α′-methyl end-capped oligothiophenes (ranging in length from the dimer to the hexamer) as suited models for different types of charge carriers in doped polythiophene, with the advantage of being free of any type of chemical or structural defect. Harada et al. have also thoroughly studied the FT-IR and FT Raman spectra of the unsubstituted oligothiophenes as a function of the chain length with the same goal.[28] These previous studies have enabled us to identify particular Raman scatterings whose peak positions and relative intensities may be used as spectroscopic markers, at the molecular scale, to evaluate the degree of quinoidization of the oligothienyl π-conjugated core induced by the oxidation of the compound to the radical cationic or dicationic form. The purpose of this work is to analyze the bunch of push−pull oligothiophenes mentioned above by means of Raman spectroscopy with the main aim of deriving information about the interaction between the π-conjugated skeleton and the electroactive end groups. Their photophysical properties and electrochemical activity are also investigated by analyzing the fluorescence emission in various solvents with different polarities and by recording their cyclic voltammograms.

II. Results and Discussion

A. Optimized Geometries. The molecular geometries of all compounds were optimized at the B3LYP/6-31G** level on the *anti* arrangement of the thienyl units and without imposing any symmetry constrains. The resulting structures were almost nearly planar, with only a very small twist angle between the two thienyl units, except for the dialkylamino or diarylamino donor groups. For all the NLO-phores, the amine nitrogen was theoretically predicted to be only slightly pyramidalized (i.e., bearing the N atom a nearly sp^2 hybridization) and with its lone electron pair almost parallel aligned to the $2p_z$ orbitals of the thienyl carbon atoms, as can be seen in the lateral view of the B3LYP/6-31G** ground-state structure of Me_2N-2T-DCV plotted in Figure 1. On the other hand, NLO-phores with a diphenylamine group are more severely twisted than their corresponding dialkylamine counterparts due to steric effects between the two pendant phenyl rings and the bithienyl π-core, lowering significantly their π-donor strength. Thus, in Ph_2N-2T-DCV, there is a dihedral angle of ca. 40° between the plane of the nearest thienyl ring and the planes formed by the N atom and the two attached C atoms of the pendant phenyl groups, whereas the corresponding angle in Me_2N-2T-DCV is close to 0°.

(20) Rao, V. P.; Wong, K. Y.; Jen, A. K.-J.; Drost, K. J. *Chem. Mater.* **1994**, *6*, 2210.
(21) (a) Brooker, L. G. S.; Keyes, G. H.; Heseltine, D. W. *J. Am. Chem. Soc.* **1951**, *73*, 5350. (b) Eckert, K.; Schröder, A.; Hartmann, H. *Eur. J. Org. Chem.* **2000**, 1327. (c) Hartmann, H.; Eckert, K.; Schröder, A. *Angew. Chem., Int. Ed.* **2000**, *39*, 556. (d) Raposo, M. M. M.; Kirsch, G. *Tetrahedron* **2003**, *59*, 4891. (e) Raposo, M. M. M.; Fonseca, M. C.; Kirsch, G. *Tetrahedron* **2004**, *60*, 4071. (f) Bedworth, P. V.; Cai, Y.; Jen, A.; Marder, S. R. *J. Org. Chem.* **1996**, *61*, 2242.
(22) (a) Zerbi, G.; Castiglioni, C.; Del Zoppo, M. In *Electronic Materials: The Oligomeric Approach*; Müllen, K., Wegner, G., Eds.; Wiley-VCH: Weinheim, Germany, 1998; p 345. (b) Castiglioni, C.; Gussoni, M.; López Navarrete, J. T.; Zerbi, G. *Solid State Commun.* **1988**, *65*, 625. (c) López Navarrete, J. T.; Zerbi, G. *J. Chem. Phys.* **1991**, *94*, 957 and 965. (d) Hernández, V.; Castiglioni, C.; Del Zoppo, M.; Zerbi, G. *Phys. Rev. B* **1994**, *50*, 9815. (e) Agosti, E.; Rivola, M.; Hernández, V.; Del Zoppo, M.; Zerbi, G. *Synth. Met.* **1999**, *100*, 101. (f) Zerbi, G. In *Handbook of Conducting Polymers*, 2nd ed.; Skotheim, T. A., Elsenbaumer, R. L., Reynolds, J. R., Eds.; Marcel Dekker: New York, 1998.
(23) Matsuzaki, S.; Moriyama, T.; Toyoda, K. *Solid State Commun.* **1980**, *34*, 857.
(24) Chappell, J. S.; Bloch, A. N.; Bryden, W. A.; Maxfield, M.; Poehler, T. O.; Cowan, D. O. *J. Am. Chem. Soc.* **1981**, *103*, 2442.
(25) Hernández, V.; Casado, J.; Ramírez, F. J.; Zotti, G.; Hotta, S.; López Navarrete, J. *J. Chem. Phys.* **1996**, *104*, 9271.
(26) Casado, J.; Hernández, V.; Hotta, S.; López Navarrete, J. *J. Chem. Phys.* **1998**, *109*, 10419.
(27) Casado, J.; Hernández, V.; Hotta, S.; López Navarrete, J. *Adv. Mater.* **1998**, *10*, 1458.
(28) Harada, I.; Furukawa, Y. In *Vibrational Spectra and Structure*; Durig, J. R., Ed.; Elsevier: Amsterdam, 1991; Vol. 19.

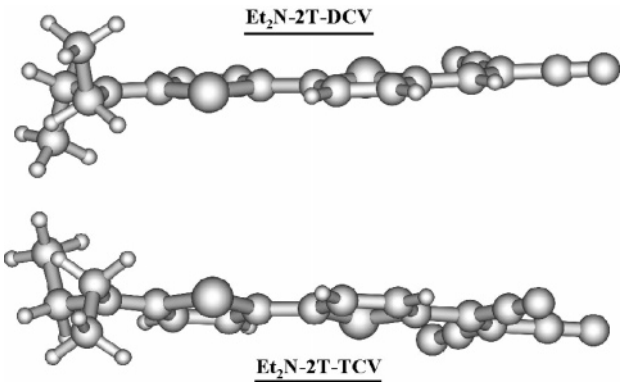

FIGURE 1. Lateral view of the optimized ground-state molecular structures of Et_2N-2T-DCV and Et_2N-2T-TCV.

To examine in a greater detail the effect of the twist of the amine group on the ground-state polarization of the π-conjugated frame, we also optimized the structure of Me_2N-2T-DCV in three different situations: (i) one in which the N lone electron pair was kept in a *anti* conformation with respect to the nearest double bond of the adjacent thiophene ring; (ii) the corresponding *syn* conformer; and (iii) one with the N lone pair pointing out of the π-conjugated frame while both N−Me bonds are kept tilted out from the bithienyl core least-squares plane by about 30° (i.e., this models a situation in which the nitrogen should bear a nearly sp^3 hybridization).

One might anticipate higher total energies for the latter three spatial orientations of the dialkylamine than for the nonconstrained structure, due to worse delocalization of the HOMO over the entire NLO-phore, as was indeed found; thus the *anti*, *syn*, and sp^3 model structures were computed to be higher in energy than the minimum energy sp^2 one by 6.53, 5.57, and 4.17 kcal mol^{-1}, respectively (i.e., the rotation around the N−C_α bond is predicted to be highly hindered in the ground state due to conjugation between the amine donor group and the π-frame). This effective conjugation is also reflected by the significant change of the ground-state dipole moment between the various model structures: 8.98 D (*anti*), 9.49 D (*syn*), 11.32 D (sp^3), and 13.19 D (minimum or near sp^2). The topologies and energies of the HOMO frontier orbital for these four models, depicted in Figure 2, illustrate more precisely the large contribution by part of the amine N atom as its lone pair is effectively allowed to freely interact with the π-system of the bithienyl spacer.

Figure 3 displays a comparison between the optimized B3LYP/6-31G** bond lengths for unsubstituted bithiophene (hereafter referred to as 2T) and for Et_2N-2T-DCV and Et_2N-2T-TCV as representative examples of each set of NLO-phores. In addition, it includes the overall NPA (natural population analysis) atomic charges over different molecular domains for the same systems. One observes that the attachment of either an electron-withdrawing DCV or TCV group at the end α-position of the bithienyl electron relay induces the appearance of a strong quinoid character over both thiophene rings (see Figure 4). Thus, as for Et_2N-2T-DCV, the double C_5=C_6 and C_7=C_8 (see atom numbering in Figure 3) bonds undergo a lengthening by about 0.018 and 0.028 Å, respectively, whereas the single C_6−C_7 bond shrinks by −0.025 Å, and for Et_2N-2T-TCV, the relevant values amount to 0.020, 0.032, and −0.029 Å, respectively. Conversely, the skeletal C_1=C_2, C_2−C_3, and C_3=C_4 bond lengths of the thienyl ring linked to the donor change by 0.026, −0.015, and 0.005 Å in the former NLO-phore and by 0.029, −0.019, and 0.008 Å in the latter one. Finally, the outermost C−S bond lengths are predicted to sizably increase by nearly 0.030 Å with respect to 2T. This lengthening, however, is reflecting three different phenomena: (i) the steric interaction between the end-capping groups and the bulky sulfur atoms; (ii) the further extension of the π-conjugation from the bithienyl electron relay toward the donor/acceptor end groups (or, in other words, the disappearance upon disubstitution of the end α,α′-positions of the chain-end effects inherent to 2T, which also justifies for the sizable lengthening of the C_1=C_2 and C_7=C_8 bonds); and (iii) the distinct role played by the two S atoms in each NLO-phore. In this regard, the B3LYP/6-31G** NPA charges on the S atoms closest to the donor and acceptor groups, respectively, amount to 0.398 and 0.485 *e* in Et_2N-2T-DCV, and 0.404 and 0.493 *e* in Et_2N-2T-TCV, whereas the corresponding value for the two symmetry-equivalent S atoms in 2T is 0.451 *e*.

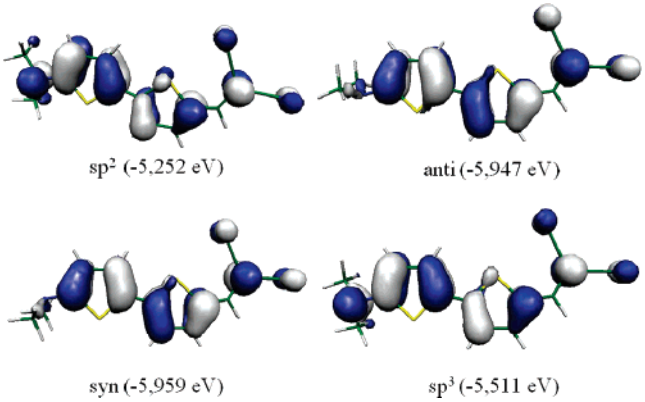

FIGURE 2. Changes in the electronic density contour (0.03 *e*/$bohr^3$) and absolute energy for the HOMO orbital of Me_2N-2T-DCV for the four different spatial orientations of the dimethylamino donor group with respect to the least-squares plane defined by the bithienyl π-conjugated electron relay.

For Et_2N-2T-DCV, the differences between the average lengths of the successive skeletal single−double CC bonds (i.e., the bond length alternation, BLA, parameter can be regarded as a measure of the degree of quinoidization) of the thienyl rings directly attached to the acceptor and donor amount to 0.003 and 0.020 Å, respectively, while the corresponding value for 2T is 0.051 Å (i.e., the BLA values for the two thienyl rings were computed in each case according to: $r(C_2C_3)$ − 0.5, $r(C_1C_2)$ − 0.5 $r(C_3C_4)$, or $r(C_6C_7)$ − 0.5 $r(C_5C_6)$ − 0.5 $r(C_7C_8)$). The differences in BLA values, as expected, are even more pronounced upon increasing acceptor strength; thus they amount to −0.005 and 0.013 Å, respectively, for Et_2N-2T-TCV (i.e., the former negative value is already indicative of the full reversal from an aromatic-like pattern to a quinoid-like one).[29]

To gain a deeper insight into the ground-state polarization of the systems, the net charges accumulated by the different constituting moieties were calculated using the NPA algorithm. As shown in Figure 3B, the net charge supported by the acceptor group in Et_2N-2T-DCV (−0.218 *e*) is much higher than that

(29) (a) Casado, J.; Miller, L. L.; Mann, K. R.; Pappenfus, T. M.; Higuchi, H.; Ortí, E.; Milián, B.; Pou-Amérigo, R.; Hernández, V.; López Navarrete, J. T. *J. Am. Chem. Soc.* **2002**, *124*, 12380. (b) Casado, J.; Pappenfus, T. M.; Mann, K. R.; Ortí, E.; Viruela, P. M.; Milián, B.; Hernández, V.; López Navarrete, J. T. *Chem. Phys. Chem.* **2004**, *5*, 529. (c) Berlin, A.; Grimoldi, S.; Zotti, G.; Malave Osuna, R.; Ruiz Delgado, M. C.; Ponce Ortiz, R.; Casado, J.; Hernández, V.; López Navarrete, J. T. *J. Phys. Chem. B* **2005**, *109*, 22308.

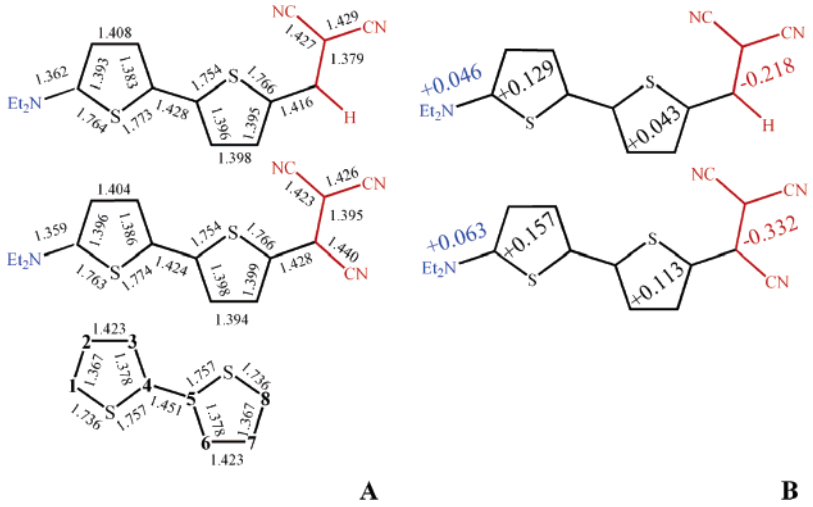

FIGURE 3. Optimized structures (A) and overall NPA charges (B) on various molecular domains for Et_2N-2T-DCV and Et_2N-2T-TCV as deduced from of their ground-state B3LYP/6-31G** molecular structures. The optimized skeletal bond lengths for 2T at the same level of theory are also reported for comparison purposes.

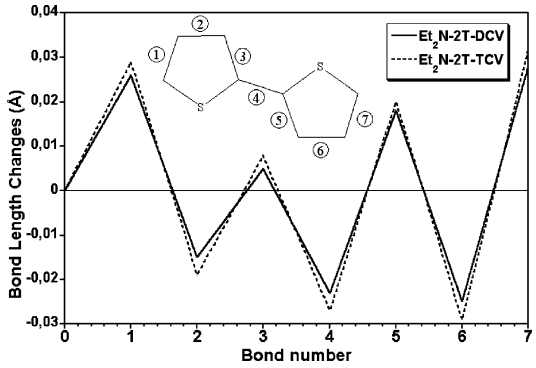

FIGURE 4. Changes of the optimized skeletal C═C/C−C bond lengths of the π-core of Et_2N-2T-DCV and Et_2N-2T-TCV relative to the corresponding B3LYP/6-31G** values for 2T.

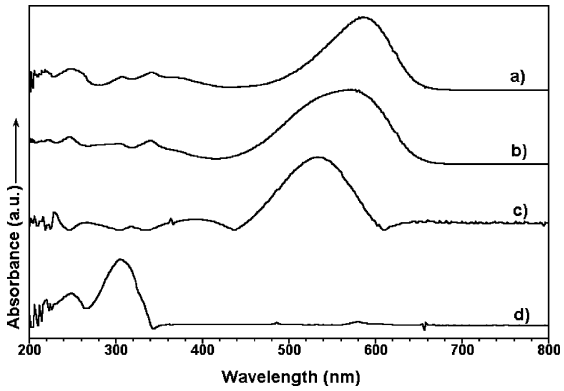

FIGURE 5. UV−Vis absorption spectra of (a) Et_2N-2T-DCV, (b) piper-2T-DCV, (c) morph-2T-DCV, and (d) 2T in CH_2Cl_2 solution.

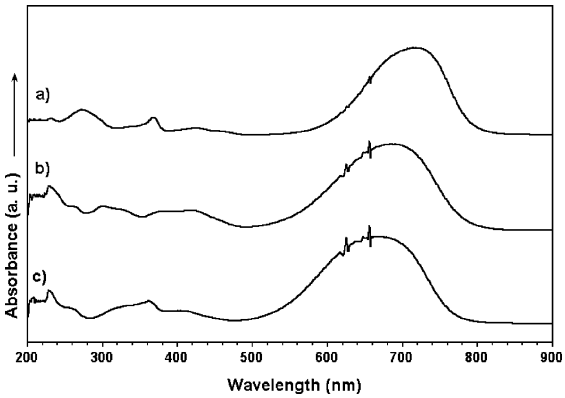

FIGURE 6. UV−Vis absorption spectra of (a) Et_2N-2T-TCV, (b) Ph_2N-2T-TCV, and (c) morph-2T-TCV in CH_2Cl_2 solution.

over the amine donor moiety (+0.046 *e*). Calculations also indicate that the negative charge over the DCV group is mainly balanced by the bithienyl π-conjugated core, which bears positive charges of +0.043 and +0.129 *e* on the thienyl rings linked to the acceptor and donor groups, respectively. Thus the strong electron-withdrawing ability of the cyanovinyl acceptors gives rise to a strong polarization of the π-conjugated backbone, lowering the aromatic character of both thienyl rings.

B. Optical Properties. 1. Absorption Spectra. As can be observed in Figures 5 and 6, the optical spectra of all the systems recorded in dichloromethane showed a broad, strong, and structureless visible absorption, with its maximum around 550 or 680 nm (i.e., for the DCV set or the TCV set, respectively). In Figure 5, the spectrum of 2T is also shown for comparison. The significant red shift of the longest wavelength absorption by about 200 nm upon donor/DCV substitution of the terminal positions and by around 130 nm upon DCV → TCV replacement clearly evidences the deeper structural/electronic modifications taking place in the π-conjugated backbones upon push−pull functionalization.

The optical properties of Et_2N-2T-DCV were investigated theoretically by calculating the lowest-energy electronic excited states using the time-dependent DFT approach. Experimentally, the UV−vis spectrum of Et_2N-2T-DCV exhibits its longest wavelength absorption at 535 nm (2.32 eV) in nonpolar solvents, such as cyclohexane. Time-dependent DFT calculations in the vacuum predict the occurrence of only one electronic transition in the visible region at 2.56 eV with an oscillator strength (*f*) of 1.00 (i.e., the closest allowed optical transition is predicted to appear at 3.63 eV, with $f = 0.15$). The transition at 2.56 eV corresponds to the $\pi-\pi^*$ excitation to the first singlet excited electronic state and is mainly described by a one-electron promotion from the highest occupied molecular orbital (HOMO)

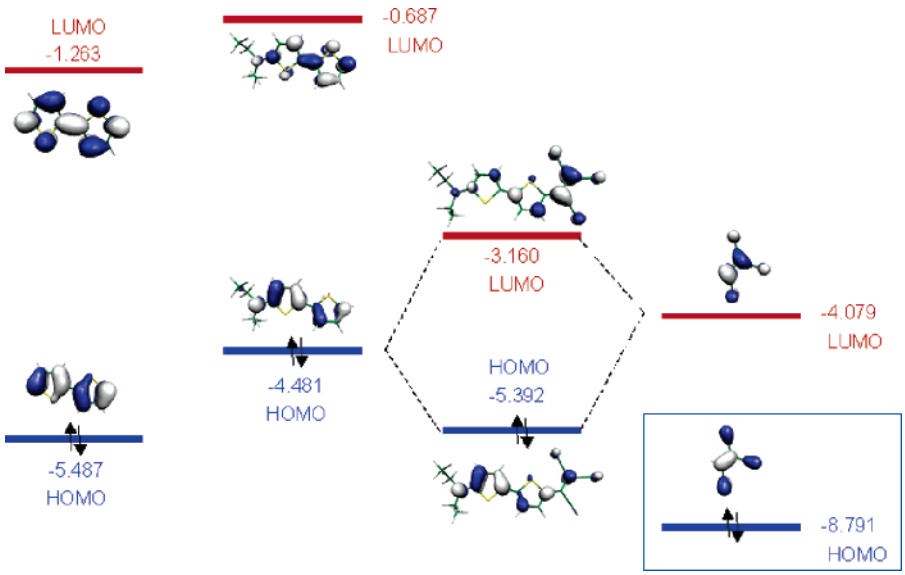

FIGURE 7. B3LYP/6-31G** molecular orbital diagram showing the coupling between the TCV-H and Et_2N-2T fragments of Et_2N-2T-TCV. The HOMO data of TCV-H in blue indicate no mixing with the frontier orbitals of Et_2N-2T. The electronic density contours (0.03 *e*/bohr^3) and absolute energies of the HOMO (blue) and LUMO (red) orbitals of 2T (left) are also shown for the sake of comparison.

to the lowest unoccupied molecular orbital (LUMO). Although both orbitals spread over the whole molecule, the HOMO displays a larger electron density around the donor group, whereas the LUMO mostly lies on the neighborhood of the dicyanovinyl group (see Figure 7). Regarding the related Et_2N-2T-TCV system, the lowest-energy $\pi-\pi^*$ vertical excitation is predicted by the single-molecule TDDFT calculations to further red shift to 2.30 eV (with $f = 0.93$), whereas the closest visible absorption should be observed near 3.36 eV, with an oscillator strength of only 0.19. Thus, the strong visible absorption band observed experimentally in each case at the longest wavelength does not have a multiconfigurational character but arises from a single electronic transition, which in its turn implies an electron density transfer from the donor subunit to the acceptor subunit. The charge-transfer nature of this optical HOMO → LUMO absorption band is further supported by the enhancement of the dipole moment associated with the electronic transition in the Et_2N-2T-DCV system, being theoretically calculated to increase from 13.2 D in the ground state to 19.9 D in the first singlet excited state, for the isolated molecule in the vacuum.

Let us go further in the understanding of the narrowing of the optical gap in Et_2N-2T-DCV and Et_2N-2T-TCV as compared with 2T. Oligothienyl chain substitution with acceptor groups gives rise to the appearance of a new empty energy level located anywhere between the original HOMO and LUMO frontier orbitals of the unsubstituted π-conjugated chain. The new energy level is related to a new molecular orbital mainly located on the acceptor group (i.e., see for instance the LUMO of Et_2N-2T-TCV in Figure 7), and its relative position steadily approaches that of the doubly occupied HOMO of the bithienyl electron relay with increasing acceptor strength. As a result, the energy required to promote one electron from the HOMO to the LUMO in the push−pull NLO-phore decreases with increasing number of CN groups in the electron-withdrawing end moiety, thus accounting for the narrowing of the optical gap from Et_2N-2T-DCV to Et_2N-2T-TCV.

Figure 7 displays the MO diagram describing the interaction between TCV-H (tricyanoethane) and the Et_2N-2T fragment. Both the HOMO and LUMO levels are stabilized in Et_2N-2T-TCV in comparison with those of Et_2N-2T (particularly in the case of the LUMO). Let us now quantitatively account for the main reasons for this behavior. To this end, it is necessary to consider the energies and topologies of the doubly occupied HOMO and empty LUMO frontier orbitals of the two interacting moieties; the extent of the interaction between their orbitals depends on two main factors: (i) the values of the linear combination of atomic orbital (LCAO) coefficients and the symmetry of the MO term (which defines the bonding or antibonding character) of the connecting C atoms; and (ii) the relative energy position (energy difference) of the two interacting levels.

Considering the HOMO of TCV-H, the largest interaction is expected to take place with doubly occupied π-molecular orbitals of Et_2N-2T of similar energies (i.e., near −8.8 eV); hence, the interaction between the TCV-H HOMO and the HOMO of Et_2N-2T is expected to be negligible. The opposite is expected to occur for the interaction between the LUMO of TCV-H and the HOMO of Et_2N-2T since they are much closer in energy. The coupling between the HOMO of Et_2N-2T and the LUMO of TCV-H thus results in the following:

(i) A doubly occupied energy level (HOMO of Et_2N-2T-TCV), resulting from their bonding interaction, with a moderate stabilization by ∼0.9 eV relative to the HOMO of Et_2N-2T.

(ii) An empty molecular orbital due to their antibonding combination, with an energy above the LUMO of TCV-H offset by 0.9 eV. The latter orbital becomes the LUMO of the Et_2N-2T-TCV NLO-phore, which in addition is largely stabilized by nearly 1.90 eV with respect to the LUMO of isolated 2T.

Furthermore, this theoretical description reveals that no significant role is played by the 2T LUMO in the LUMO of Et_2N-2T-TCV, at the time that it also highlights two interesting points: (i) the HOMO of Et_2N-2T-TCV is mainly accounted for by the bithienyl electron relay (2T HOMO energy of −5.487 eV and Et_2N-2T-TCV HOMO energy of −5.392 eV); and (ii) the LUMO of Et_2N-2T-TCV is mainly accounted for by the tricyanovinyl moiety (TCV-H LUMO energy of −4.079 eV and Et_2N-2T-TCV LUMO energy of −3.160 eV). As another result, from the interaction between the HOMO of Et_2N-2T and the

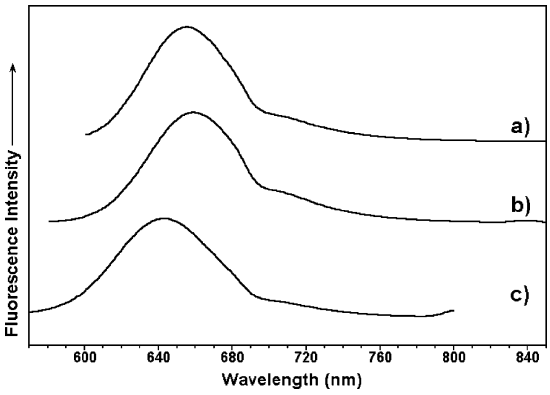

FIGURE 8. Fluorescence emission spectra of (a) Et_2N-2T-DCV, (b) piper-2T-DCV and, (c) morph-2T-DCV in CH_2Cl_2 solution.

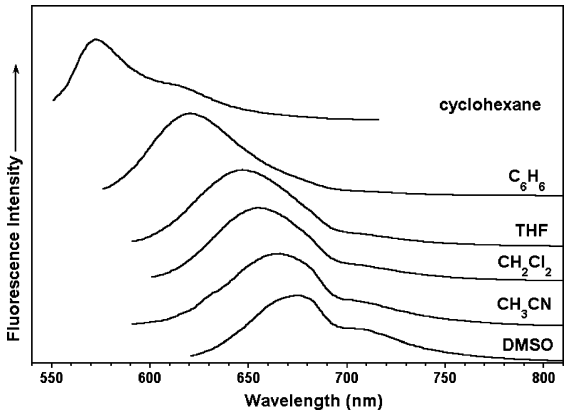

FIGURE 9. Fluorescence spectra of Et_2N-2T-DCV in solvents of varying polarity. Excitation wavelength in each case corresponds to the absorption maximum.

LUMO of TCV-H, a certain Et_2N-2T → TCV electron density polarization can be anticipated to occur, as a consequence of the partial occupation of the empty orbital of the acceptor at the expense of the doubly occupied HOMO of Et_2N-2T. This fact outlines the sizable donor−acceptor interaction that accounts for the ground-state electronic structure of these NLO-phores, and which will have important consequences on their electrochemical and vibrational properties (vide infra). Another interesting distinction is that the HOMO → LUMO electronic excitation really corresponds to a virtual displacement of the electron density from the electron-rich side of the chromophore to the electron-deficient one, that is, a charge-transfer (CT) exciton with seemingly effective electron−hole separation.

2. Emission Spectra. Fluorescence spectra of some representative DCV chromophores in dichloromethane solution are depicted in Figure 8. All the members of the DCV set show similar emission patterns, with maxima close to 650 nm in CH_2Cl_2 solution. Although dual fluorescence was not observed in any case (i.e., what should be indicative of the occurrence of largely twisted intramolecular charge-transfer states, TICTs),[30] the weak fluorescence emissions experimentally recorded at the longer wavelength might be tentatively assigned to an equilibrium between various planar conformational isomers upon excitation of the $\pi-\pi^*$ transition of the NLO-phore (i.e., *cis* and *anti* arrangements of thienyl units have been reported to coexist in solid state for a related 3T−TCV compound).[31]

There occurs a pronounced red shift of the HOMO−LUMO absorption band on going from morph-2T-DCV (536 nm) to piper-2T-DCV (571 nm) and Et_2N-2T-DCV (585 nm). The red shift of the $\pi-\pi^*$ absorption to longer wavelengths for the diethylamine NLO-phore might be related to some steric hindrance between the two types of cyclic amines and the nearest thienyl unit, causing a rotation about the C−N bond and, consequently, to a less efficient orbital overlapping between the donor group and the bithienyl electron relay. The effect is much more noticeable for the morpholine derivative. Our data are in agreement with those already reported for the strong influence on the thiophene ^1H chemical shift (i.e., ^1H NMR spectra) of bithiophenes with alkyl (i.e., methyl and ethyl) or heterocyclic (i.e., morpholino group) amine substituents as the donor units. This effect was attributed to the steric interaction between the thiophene ring and the α-methylene of the amine, which in turn influences the interaction of the free electron pair on the nitrogen with the π-electron system.[32] Regarding their fluorescence features, nearly the same wavelengths are measured for Et_2N-2T-DCV (655 nm) and piper-2T-DCV (658 nm), at the time, the emission maximum for morph-2T-DCV (644 nm) is closer to those of the other two NLO-phores than the separation already evidenced between their respective UV−vis absorptions. Assuming a charge-transfer emissive state, full planarization of the donor/acceptor end moieties relative to the quinoidized bithienyl electron relay is presumably expected to occur upon excitation of the $\pi-\pi^*$ absorption. In such a case, full conjugation between the amine N atom (i.e., regardless of its surrounding) and the bithienyl acceptor part of the chromophore likely takes place, thus leading to quite similar fluorescence emission spectra for the whole DCV set of NLO-phores.

As for Et_2N-2T-DCV, both the absorption and fluorescence spectra are found to display a significant positive solvatochromic behavior, particularly remarkable in the case of the emission features (Figure 9), with increasing dielectric constant of the solvent. This observation is in agreement with the aforementioned photoinduced charge transfer or charge-separated emissive state, for which a steadily higher stabilization in increasingly polar solvents should be anticipated.

On going from Et_2N-2T-DCV to Et_2N-2T-TCV, however, the fluorescence emission is fully quenched. Two main routes for nonradiative decay play a main role in the photophysics of thiophene-based molecules. First, the presence of heavy sulfur atoms promotes effective spin−orbit coupling and inter-system crossing to the triplet manifold, which is believed to be the main source for nonradiative decay for the α-oligothiophenes. However, for Et_2N-2T-DCV and Et_2N-2T-TCV, the sulfur statistical weight is roughly the same, and thus the fluorescence quenching evidenced for the second system must be related to the significant narrowing of the S_0-S_1 gap, which favors the internal conversion as the main deactivation channel. The formation of nonfluorescent twisted ICT states to account for this emission quenching upon increasing strength of the donor/acceptor units might not be fully discarded.[33]

(30) (a) Retting, W.; Maus, M. In *Conformational Analysis of Molecules in Excited States*; Waluk, J., Ed.; Wiley-VCH: New York, 2000; Chapter 1, pp 1−55. (b) Grabowski, Z. R.; Rotkiewicz, K. *Chem. Rev.* **2003**, *103*, 3899. (c) Yang, J.-S.; Liau, K.-L.; Wang, C.-M.; Hwang, C.-Y. *J. Am. Chem. Soc.* **2004**, *126*, 12325.

(31) Casado, J.; Hernández, V.; Ruiz Delgado, M. C.; López Navarrete, J. T.; Pappenfus, T. M.; Williams, N.; Stegner, W. J.; Johnson, J. C.; Edlund, B. A.; Janzen, D. E.; Mann, K. R.; Orduna, J.; Villacampa. B. *Chem.—Eur. J.* **2006**, *12*, 5458.

(32) Radeglia, R.; Hartmann, H.; Scheithauer, S. *Z. Naturforsch.* **1969**, *24B*, 286.

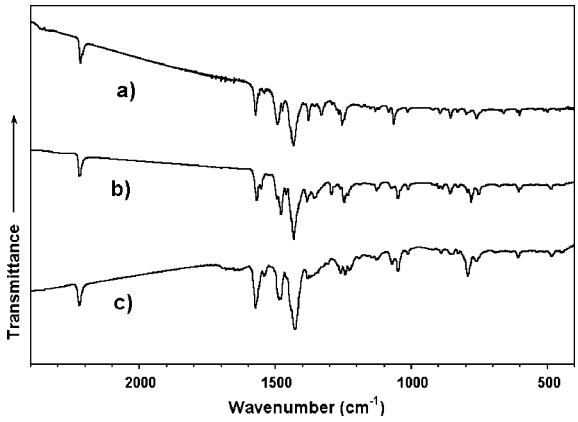

FIGURE 10. Fourier transform infrared spectra of (a) piper-2T-DCV, (b) piper-3T-DCV, and (c) piper-4T-DCV over probe energies of 2400−400 cm^{-1}.

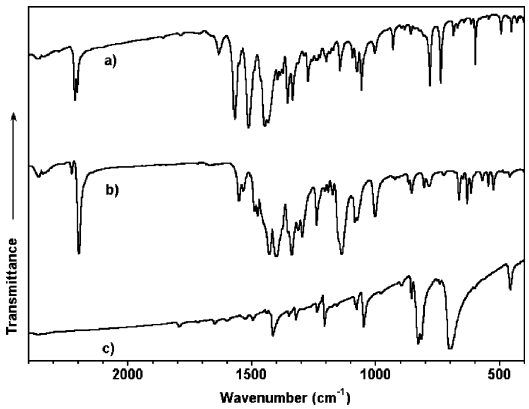

FIGURE 11. Fourier transform infrared spectra of (a) Et_2N-2T-DCV, (b) Et_2N-2T-TCV, and (c) 2T over probe energies of 2400−400 cm^{-1}.

C. Vibrational Spectra. (i) The Fourier transform infrared spectra recorded for piper-2T-DCV, piper-3T-DCV, and piper-4T-DCV in the 2400−400 cm^{-1} region are shown in Figure 10, whereas Figure 11 displays those recorded for Et_2N-2T-DCV and Et_2N-2T-TCV together with the spectrum of 2T. The complete assignment of the whole set of vibrational spectra to particular vibrations is beyond the scope of our analysis. We will restrict our further discussion only to the more relevant observations of general validity for the class of push−pull π-conjugated chromophores:

(ii) The IR (and the Raman) spectra display much more bands than for the neutral forms of symmetrically end-capped α,α′-oligothiophenes due, among other factors, to the lowering of molecular symmetry.[25]

(iii) The IR absorptions of push−pull chromophores are significantly stronger than those observed for nonpolar oligothiophenes due to the large dipole moment changes induced by the molecular vibrations, particularly, for the bands appearing between 1600 and 1400 cm^{-1}. This is quite evident for the various push−pull oligothiophenes shown in Figures 10 and 11, for which the relative intensities of the ν(C═C) stretching modes of the π-conjugated skeleton are appreciably stronger than the remaining IR-active vibrations. In addition, the replacement of the DCV acceptor group by TCV further red shifts the strongest infrared absorptions toward lower frequencies, as shown in Figure 11.

(iv) The IR and Raman spectra of a given push−pull chromophore show many similarities, both in the peak positions and in the relative intensities of the different vibrational features, while the IR and Raman spectra of nonpolar oligothiophenes (either symmetrically or asymmetrically substituted) are complementary, so that the strongest IR absorptions display a vanishing Raman intensity, and vice versa. The Raman spectra of aromatic nonpolar oligothiophenes usually display very few lines with an overwhelming intensity because of the occurrence of significant polarizability changes of the π-conjugated path along particular totally symmetric skeletal vibrations, which are commonly termed as *collective ECC modes*.[22] In the case of push−pull π-conjugated chromophores, these ECC modes become also strongly activated in the infrared because of the strong polarization of the molecular backbone induced by the attachment of two electroactive end groups, so that the initially IR-silent totally symmetric ECC modes now give rise to quite large fluxes of charge along the alternating sequence of conjugated C═C/C−C bonds, gaining consequently a strong IR activity.

The ν(CN) stretching vibrations are recorded as sharp and strong absorptions between 2220 and 2200 cm^{-1}, for most of the compounds as a well-resolved doublet. As for the DCV series, theory nicely predicts the experimentally observed two-peak structure and assigns the higher-frequency component to a normal mode in which both CN bonds vibrate in-phase and with similar amplitudes, while the lower-frequency IR absorption arises from the related out-of-phase vibrational mode. The latter ν(CN) IR feature additionally downshifts and becomes stronger upon replacing the DCV acceptor by the TCV one (as can be seen in Figure 11), due to the increasing strength of the acceptor moiety.

The frequency of the ν(CN) mode in TCNQ is known to be quite sensitive to the electron density borne by each of its four nitrile groups and downshifts either upon complexation with electron donors, such as TTF, or reduction, due to the steady lengthening of the C≡N bonds and loss of triple bond character.[34,35] Taking a quaterthienoquinodimethane as a reference, for which the ν(CN) infrared absorption is observed in the neutral state as a sharp feature at 2206 cm^{-1},[29a] we observe that the related ν(CN) IR bands appear at similar or even lower frequencies for the push−pull systems under study: piper-2T-DCV (2218 cm^{-1}), Et_2N-2T-DCV (2214 and 2204 cm^{-1}), and Et_2N-2T-TCV (2197 cm^{-1}). The large involvement of the nitrile groups in the overall ICT is also clearly evidenced by the fairly large downshift, by around 50 cm^{-1}, of the Raman-active ν(CN) stretching modes of Me_2N-2T-DCV, piper-2T-DCV, and morph-2T-DCV, as compared with the 2265 cm^{-1} frequency value measured for a nonconjugated dicyanomethane model system (see Figure 12).

Figure 13 shows a comparison between the Raman spectral profiles of Me_2N-2T-DCV recorded in the form of a pure solid sample and as dilute solutions in CH_2Cl_2 and DMSO (i.e., after properly subtracting the Raman scatterings of the corresponding solvent). It can be noticed that the vibrational spectral finger-

(33) Haucke, G.; Czerney, P.; Steen, D.; Retting, W.; Hartmann, H. *Ber. Bunsen-Ges. Phys. Chem.* **1993**, *97*, 561.

(34) (a) Takenaka, T. *Spectrochim. Acta, A* **1971**, *27*, 1735. (b) Girlando, A.; Pecile, C. *Spectrochim. Acta, A* **1973**, *29*, 1859. (c) Faulques, E.; Leblanc, A.; Molini, P.; Decoster, M.; Conan, F.; Guerchais, J. E.; Sala-Sala, J. *Spectrochim. Acta, A* **1995**, *51*, 805.

(35) Khatkale, M. S.; Devlin, J. P. *J. Chem. Phys.* **1979**, *70*, 1851.

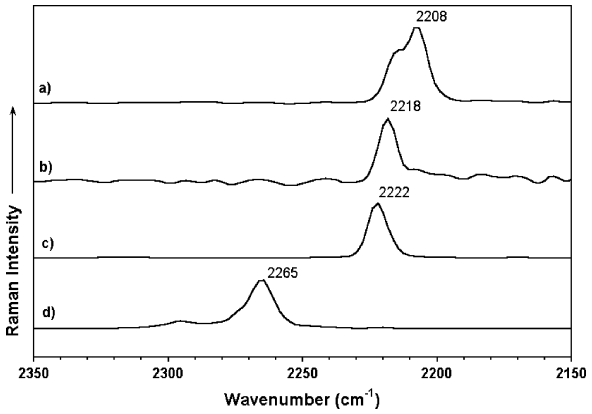

FIGURE 12. Raman bands due to the ν(CN) stretching modes of (a) Me_2N-2T-DCV, (b) piper-2T-DCV, (c) morph-2T-DCV, and (d) $CH_2(CN)_2$ as pure solid samples.

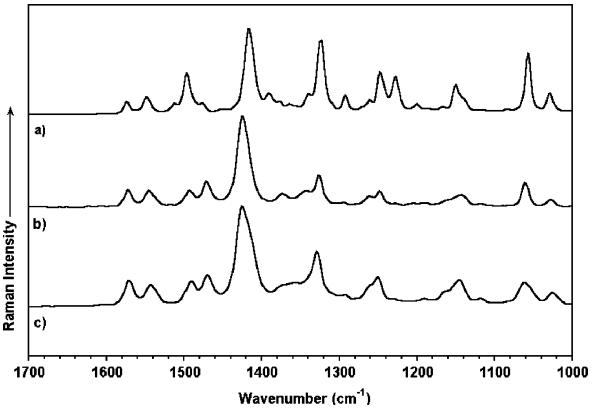

FIGURE 13. Raman spectral profiles of Me_2N-2T-DCV (a) as a pure solid sample, (b) in dilute CH_2Cl_2 solution, and (c) dilute DMSO solution, in the 1700−1000 cm^{-1} Raman shift spectral ranges.

prints of the two solutes closely resemble that collected for the pure solid. In this regard, main differences in the peak positions of the stronger Raman features do not exceed from a 6 cm^{-1} Raman blue shift in solution. It must also be noted that relative intensities of the main Raman scatterings in the three different environments are nearly the same.

These spectroscopic observations suggest that there is not a significant change in the ground-state polarization of the π-conjugated backbone on going from solids to solutions, and

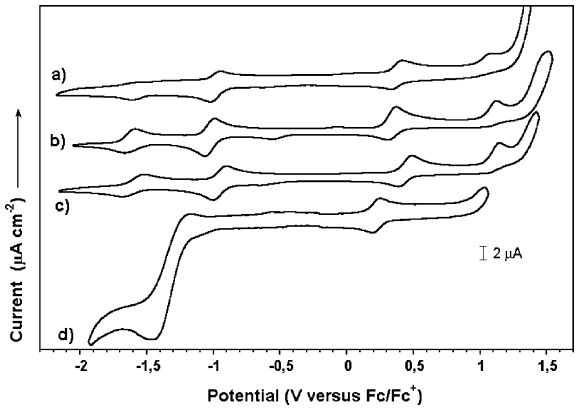

FIGURE 14. Cyclic voltammograms of (a) morph-2T-TCV, (b) Et_2N-2T-TCV, (c) Ph_2N-2T-TCV, and (d) Et_2N-2T-DCV.

that the donor/acceptor end groups should undergo only small conformational distortions upon the removal of the solid-state packing forces, when solute−solvent interactions come into play (i.e., the highly hindered rotation of the various constituting moieties about the inter-ring bonds once the crystal packing forces have been switched off constitutes another experimental evidence of the substantial degree of quinoidization of the π-conjugated frame in these NLO-phores).

D. Electrochemical Properties. Figure 14 shows the cyclic voltammetry waves recorded for some representative systems. The electrochemical response of the TCV compounds consists of stable anodic and cathodic processes, and thus all of them display a dual or amphoteric redox behavior.[36] Two reversible reductions with appreciable current densities are observed.

The first reduction process near −1.00 V is always more intense than that at higher energies (i.e., more negative potentials). Assuming a large involvement of the TCV moiety in both cathodic processes, provided its strong electron-withdrawing nature, one can relate at first sight the reduction at −1.00 V to the geminal external $(CN)_2$ groups, whereas the second reduction seemingly involves mainly the cross-conjugated CN group (i.e., this group adds a new cross-conjugated path between the bithienyl electron relay and the vinyl-geminal-dicyano acceptor). Chart 2 depicts schematically the structure of the electrochemically generated species formed along both the oxidation and reductions waves. Furthermore, both reduction processes result in being almost independent of the chemical nature of the donor moiety (see Chart 2), as expected due to

CHART 2. Species Generated in the Electrochemical Processes of Et_2N-2T-TCV[a]

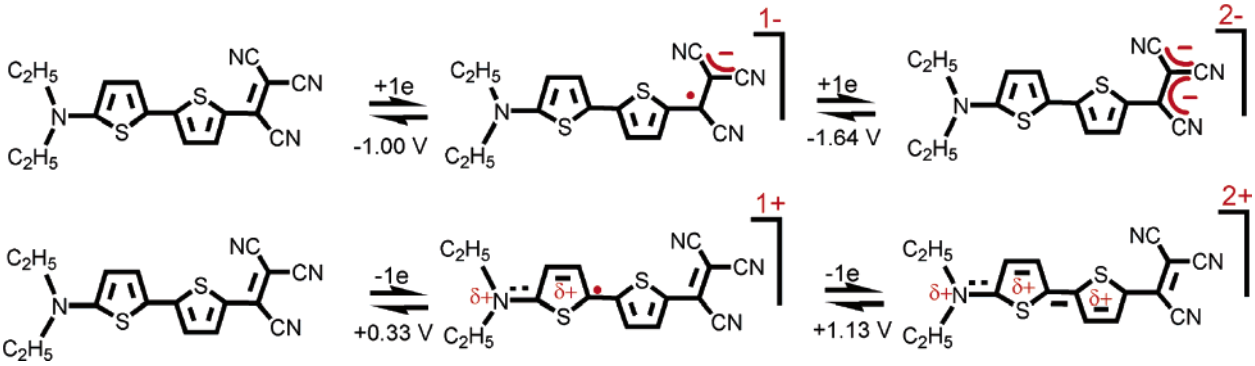

[a] Electrochemical potentials are also shown. Charge distributions for the various redox species have been derived from B3LYP or UB3LYP/6-31G** calculations.

their far location on the opposite side of the π-conjugated backbone. In line with this reasoning (Chart 2), negative charges in the anionic species are mainly concentrated in the vicinity of the CN-bearing moieties; hence for the anion of the DCV derivative (i.e., Et2N-2T-DCV), the C(H) atom connecting the dicyano and the bithiophene group (i.e., radical character) might react with other radical anions by forming dimer molecules by generation of new C−C bonds. This step is blocked when this C atom is substituted with a CN group as in the TCV derivatives. Therefore, the formation of a new C−C bond might be speculated as the mechanism lying in the observed irreversibility for the DCN molecules. When the cation radical is formed in the oxidation, the positive charge and the radical are concentrated in the donor group, so that no chemical activity is expected for the DCV group addressing the detected reversibility in the anodic branch of the electrochemical experiment.

As for the anodic branches, reversible oxidations occur near 0.4 V, followed by irreversible processes near 1.1 V. A third irreversible oxidation process is also seen for Et2N-2T-TCV and Ph2N-2T-TCV, close to the electrolyte discharge. Upon one-electron extraction in the first oxidation wave, the generated monocationic species likely spreads over the donor bithienyl half-molecule, readily mitigating the electrophilic character of the positive charge in excess. However, the subsequent extraction of the second or successive electrons leads to the appearance of electrostatic repulsions with the already-existing monocation, so that the further spatial extension of the newly injected positive charges toward the electron-deficient TCV moiety gives rise to an irreversible behavior for the second anodic wave (i.e., chemical degradation).

Within the Koopman's approach, one can correlate the energies of the HOMO/LUMO orbitals with the measured oxidation/reduction potentials (i.e., oxidation consists of an electron extraction from the doubly occupied HOMO, whereas electrons are added to the empty LUMO upon reduction). In this regard, the main location of the electron densities related to the HOMO and LUMO frontier orbitals (see Figure 6) over the amine-bithienyl and the bithienyl-TCV molecular domains, respectively, agrees well with the above assignments of the redox processes.

As already mentioned, a quite different electrochemical response upon reduction is observed going from the TCV compounds to the DCV ones. The main cathodic process for the latter class of materials is now fully irreversible. On the other hand, however, the anodic profile is found to be still rather similar for both morph-2T-DCV and morph-2T-TCV, thus supporting the aforementioned view about the strong location of this redox process over the amine-bithienyl part of the chromophore. In this regard, we see that the first oxidation potential moderately shifts, by only 0.1 V, to higher energies upon the attachment of the third CN group to the acceptor group, which indeed reflects the relatively small reduction of the electron donor ability of the TCV−NLO-phores with respect to their DCV counterparts.

III. Conclusions

We have reported on a comprehensive analysis of two sets of push−pull NLO-phores built around a π-conjugated bithienyl electron relay and bearing various types of amino donor groups and either a dicyanovinyl (DCV) or tricyanovinyl (TCV) moiety as the acceptor. All the compounds show interesting electronic characteristics, although the tricyanovinyl counterparts possess more favorable properties in that the electronic absorption maxima are very much shifted to the longer wavelength regions. Et_2N-2T-DCV and Et_2N-2T-TCV are representative examples providing guidelines for the whole interpretation of the optical, electrochemical, and conjugational properties of both sets of molecules.

The molecular geometry optimizations reveal a substantial degree of quinoidization of the π-conjugated backbone of both sets of NLO-phores, with a full reversal of the geometry of the thienyl ring linked to the TCV acceptor group from an aromatic-like pattern to a quinoid-like one. Furthermore, the B3LYP/6-31G** NPA atomic charge distribution also indicates that the net charge over the DCV or TCV acceptor moiety is substantially higher than the overall charge on the amine donor group, and that the π-conjugated electron relay is strongly polarized since it bears nearly 70% of the net positive charge of the zwitterionic form of the NLO-phore.

All the D−π−A systems studied in this paper showed an intramolecular charge-transfer band in their visible absorption spectra, whose position is influenced both by the nature of the end groups and the polarity of the solvent. The topologies and energies of the molecular orbitals were studied by means of TDDFT//B3LYP/6-31G**, showing that the HOMO−LUMO energy gaps account for the observed intramolecular charge transfer from the donor subunit to the acceptor subunit.

The compounds have been also analyzed by means of IR and Raman spectroscopies in solid state as well as in a variety of solvents. As a first result, the great resemblance between the IR and Raman spectral profiles constitutes a proof of a very effective intramolecular charge transfer. The π-conjugated skeleton gives rise to collective normal vibrational modes during which changes of the molecular polarizability are quite sizable. In the case of push−pull chromophores, these vibrational modes also become very strong in the IR spectra because of the high polarization of the molecular frame induced by the presence of the two polar end groups. The large intensities of these IR-active modes can be ascribed to large fluxes of charge along the alternating sequence of C═C/C−C bonds, which generate a very large molecular dipole moment variation directed along the chain axis. Very subtle Raman spectral changes between solutes and solids were noticed for all the NLO-phores. This experimental finding suggests that the effective π-conjugation in these push−pull oligothiophenes is the driving force which determines that the conformational distortions of the thienyl rings and end groups out of coplanarity must be very small even in solution.

The electrochemical behavior of the two sets of chemicals has been well documented. All the compounds were found to display an amphoteric redox response. The first oxidation leads to stable monocationic species in all the cases, but the subsequent electron extractions give rise to an irreversible behavior for the second anodic feature, which is likely related to the quite short chain length of the compounds. Regarding the cathodic waves, while the TCV compounds display two well-separated reversible reductions, the main cathodic process for the DCV products is found, however, to be fully irreversible.

Finally, density functional theory has been shown to provide support for the observed electronic and optical properties of

(36) Dealing with 1 mM solutions, no signals due to the isolated 0.1 M $TBAPF_6/CH_2Cl_2$ electrolyte appear in the CV experiments. No clear insights are found (i.e., adsorption/desorption processes) about the weak processes around −0.5 and 0.00 V (especially distinguished in CV labeled as b).

the systems studied in this work, offering excellent correlations with the measured quantities. The power and usefulness of both DFT and TDDFT model chemistry calculations have been thus well documented. The present study offers opportunity for further development of novel functional organic materials for electronic applications in addition to providing a basic understanding of the mechanisms governing the electron-transfer processes in π-conjugated donor−acceptor arrays.

IV. Experimental Section

Chart 1 displays the chemical structures and abbreviated notation of the push−pull oligothiophenes of this study, which were prepared according to the following citations: Me_2N-2T-DCV in 12c and 21d; Et_2N-2T-DCV in 21b and 21d; Et_2N-2T-TCV in 21b and 21d; Ph_2N-2T-DCV in 21f; morph-2T-DCV in 21b; morph-2T-TCV in 21b; piper-2T-DCV in 21d and 21f; piper-3T-DCV in 21e; and piper-4T-DCV in 21e.

Fourier transform infrared absorption (FT-IR) spectra were recorded on KBr pellets. FT-IR spectra, with a spectral resolution of 2 cm^{-1}, were collected as the average of 50 scans. Interference from atmospheric water vapor was minimized by purging the instrument with dry argon before starting the data collection. FT Raman scattering spectra were collected using a Nd:YAG laser source (λ_{exc} = 1064 nm), in a backscattering configuration. The operating power for the exciting laser radiation was kept to 100 mW in all the experiments. Samples were analyzed as pure solids in sealed capillaries and dilute solutions with solvents of the highest analytical quality. Typically, 1000 scans with 4 cm^{-1} spectral resolution were averaged to optimize the signal-to-noise ratio. In the emission experiments, no fluorescent contaminants were detected upon excitation in the wavelength region of experimental interest. Solutions were prepared with an absorbance between 0.1 and 0.2 at the excitation wavelength.

Cyclic voltammetries of the neutral compounds were carried out at room temperature between −2.00 and 1.5 V, at a scan rate of 100 mV/s, using a 0.1 M tetrabutylammonium hexafluorophosphate ($TBAPF_6$) solution in dichloromethane; 1 mM solutions of the compounds were used in all the cases. Solutions were deaerated by N_2 bubbling prior to each measurement, which also were run under a continuous N_2 gas flow. A glassy carbon electrode and a platinum wire were employed as working and auxiliary electrodes, respectively. A Ag/AgCl electrode was used as reference, which was checked against ferrocene/ferrocenium couple (Fc/Fc^+) before and after each experiment.

Density functional theory (DFT) calculations were carried out by means of the Gaussian 03 program[37] running on a SGI Origin 2000 supercomputer. We used Becke's three-parameter exchange functional combined with the LYP correlation functional (B3LYP).[38] It has already been shown that the B3LYP functional yields similar geometries for medium-sized molecules as MP2 calculations do with the same basis sets.[39,40] Moreover, the DFT force fields calculated using the B3LYP functional yield infrared spectra in very good agreement with experiments.[41,42] We also made use of the standard 6-31G** basis set.[43] Optimal geometries were determined on isolated entities. All geometrical parameters were allowed to vary independently apart from planarity of the rings. On the resulting ground-state optimized geometries, harmonic vibrational frequencies and infrared and Raman intensities were calculated numerically with the B3LYP functional. Natural population analysis (NPA) was carried out to compute atomic charges.[44]

We used the often-practiced adjustment of the theoretical force fields in which calculated harmonic vibrational frequencies are uniformly scaled down by a factor of 0.96 for the 6-31G** calculations, as recommended by Scott and Radom.[41] This scaling procedure is often accurate enough to disentangle serious experimental misassignments. All quoted vibrational frequencies reported in this paper are thus scaled values. The theoretical spectra were obtained by convoluting the scaled frequencies with Gaussian functions (10 cm^{-1} width at the half-height). The relative heights of the Gaussians were determined from the theoretical Raman scattering activities.

Vertical electronic excitation energies were computed by using the time-dependent DFT (TDDFT) approach.[45,46] The 20 lowest-energy electronic excited states were at least computed for all the molecules. The computational cost of TDDFT is roughly comparable to that of single-excitation theories based on a HF ground state, such as single-excitation configuration interactions (CIS). Numerical applications reported so far indicate that the TDDFT formalism employing current exchange-correlation functionals performs significantly better than HF-based single-excitation theories for the low-lying valence excited states of both closed-shell and open-shell molecules.[47,48] TDDFT calculations were carried out using the B3LYP functional and the 6-31G** basis set on the previously optimized molecular geometries obtained at the same level of calculation. Molecular orbital contours were plotted using Molekel 4.3.[49]

Acknowledgment. Research at the University of Málaga was supported by the Ministerio de Educación y Ciencia (MEC) of Spain through project BQU2003-03194, and by the Junta de Andalucía for funding our FQM-0159 scientific group. J.C. is grateful to the Ministerio de Ciencia y Tecnología of Spain for a Ramón y Cajal position of Chemistry at the University of

(37) Frisch, M. J.; Trucks, G. W.; Schlegel, H. B.; Scuseria, G. E.; Robb, M. A.; Cheeseman, J. R.; Montgomery, J. A., Jr.; Vreven, T.; Kudin, K. N.; Burant, J. C.; Millam, J. M.; Iyengar, S. S.; Tomasi, J.; Barone, V.; Mennucci, B.; Cossi, M.; Scalmani, G.; Rega, N.; Petersson, G. A.; Nakatsuji, H.; Hada, M.; Ehara, M.; Toyota, K.; Fukuda, R.; Hasegawa, J.; Ishida, M.; Nakajima, T.; Honda, Y.; Kitao, O.; Nakai, H.; Klene, M.; Li, X.; Knox, J. E.; Hratchian, H. P.; Cross, J. B.; Adamo, C.; Jaramillo, J.; Gomperts, R.; Stratmann, R. E.; Yazyev, O.; Austin, A. J.; Cammi, R.; Pomelli, C.; Ochterski, J. W.; Ayala, P. Y.; Morokuma, K.; Voth, G. A.; Salvador, P.; Dannenberg, J. J.; Zakrzewski, V. G.; Dapprich, S.; Daniels, A. D.; Strain, M. C.; Farkas, O.; Malick, D. K.; Rabuck, A. D.; Raghavachari, K.; Foresman, J. B.; Ortiz, J. V.; Cui, Q.; Baboul, A. G.; Clifford, S.; Cioslowski, J.; Stefanov, B. B.; Liu, G.; Liashenko, A.; Piskorz, P.; Komaromi, I.; Martin, R. L.; Fox, D. J.; Keith, T.; Al-Laham, M. A.; Peng, C. Y.; Nanayakkara, A.; Challacombe, M.; Gill, P. M. W.; Johnson, B.; Chen, W.; Wong, M. W.; Gonzalez, C.; Pople, J. A. *Gaussian 03*, revision B.04; Gaussian Inc.: Pittsburgh, PA, 2003.

(38) Becke, A. D. *J. Chem. Phys.* **1993**, *98*, 1372.

(39) Stephens, P. J.; Devlin, F. J.; Chabalowski, F. C. F.; Frisch, M. J. *J. Phys. Chem.* **1994**, *98*, 11623.

(40) Novoa, J. J.; Sosa, C. *J. Phys. Chem.* **1995**, *99*, 15837.

(41) Scott, A. P.; Radom, L. *J. Phys. Chem.* **1996**, *100*, 16502.

(42) Rauhut, G.; Pulay, P. *J. Phys. Chem.* **1995**, *99*, 3093.

(43) Francl, M. M.; Pietro, W. J.; Hehre, W. J.; Binkley, J. S.; Gordon, M. S.; Defrees, D. J.; Pople, J. A. *J. Chem. Phys.* **1982**, *77*, 3654.

(44) (a) Reed, A. E.; Weinstock, R. B.; Weinhold, F. *J. Chem. Phys.* **1985**, *83*, 735. (b) Reed, A. E.; Curtiss, L. A.; Weinhold, F. *Chem. Rev.* **1988**, *88*, 899. (c) Weinhold, F. In *Encyclopedia of Computational Chemistry*; Schleyer, P. v. R., Ed.; Wiley: New York, 1998; Vol. 3. (d) Hameka, H. F. *Mol. Phys.* **1958**, *1*, 203. (e) Ditchfield, R. *Mol. Phys.* **1974**, *27*, 789.

(45) (a) Runge, E.; Gross, E. K. U. *Phys. Rev. Lett.* **1984**, *52*, 997. (b) Gross, E. K. U.; Kohn, W. *Adv. Quantum Chem* **1990**, *21*, 255. (c) *Density Functional Theory*; Gross, E. K. U., Driezler, R. M., Eds.; Plenum Press: New York, 1995; p 149.

(46) Casida, M. E. *Recent Advances in Density Functional Methods, Part I*; Chong, D. P., Ed.; World Scientific: Singapore, 1995; p 115.

(47) Koch, W.; Holthausen, M. C. *A Chemist's Guide to Density Functional Theory*; Wiley-VCH: Weinheim, Germany, 2000.

(48) Casado, J.; Miller, L. L.; Mann, K. R.; Pappenfus, T. M.; Kanemitsu, Y.; Ortí, E.; Viruela, P. M.; Pou-Amérigo, R.; Hernández, V.; López Navarrete, J. T. *J. Phys. Chem. B* **2002**, *106*, 3872.

(49) Portmann, S.; Lüthi, H. P. *Chimia* **2000**, *54*, 766−770.

Málaga. The group at the University of Minho acknowledges the Foundation for Science and Technology (Portugal) for financial support through Centro de Química (UM) and through POCTI, FEDER (ref. POCTI/QUI/37816/2001). M.M.M.R. and A.M.C.F. are also grateful to Professor G. Kirsch from the University of Metz (France) for his collaboration.

Supporting Information Available: Tables S1−S13 provide the B3LYP/6-31G** Cartesian coordinates for the optimized geometries and total formation energies for all the theoretically modeled molecules, including neutrals, cations, and anions. This material is available free of charge via Internet at http://pubs.acs.org.

JO060318V